Angewandte Chemie
GDCh
Eine Zeitschrift der Gesellschaft Deutscher Chemiker
www.angewandte.de

Akzeptierter Artikel

Titel: Fluorescence Quenching Effects of Tetrazines and Their Diels-Alder Products: Mechanistic Insight Toward Fluorogenic Efficiency

Autoren: Brismar Pinto-Pacheco, William Paul Carbery, Sameer Khan, Daniel B Turner, and Daniela Buccella

Zitierweise: *Angew. Chem. Int. Ed.* 10.1002/anie.202008757

Link zur VoR: https://doi.org/10.1002/anie.202008757

WILEY-VCH

10.1002/ange.202008757

RESEARCH ARTICLE

WILEY-VCH

Fluorescence Quenching Effects of Tetrazines and Their Diels-Alder Products: Mechanistic Insight Toward Fluorogenic Efficiency

Brismar Pinto-Pacheco,[a] William P. Carbery,[a] Sameer Khan,[a] Daniel B. Turner*[a][b] and Daniela Buccella*[a]

[a] Dr. B. Pinto-Pacheco, Dr. W. P. Carbery, S. Khan, Prof. Dr. D. B. Turner, Prof. Dr. D. Buccella
Department of Chemistry
New York University
100 Washington Square East, New York, NY 10003, USA.
E-mail: dbuccella@nyu.edu (D.B.)

[b] Current address: Micron School of Materials Science and Engineering
Boise State University
Boise, ID 83725, USA
E-mail: danielturner926@boisestate.edu (D.B.T.)

Supporting information for this article is given via a link at the end of the document.

Abstract: Inverse electron demand Diels–Alder (iedDA) reactions between *s*-tetrazines and strained dienophiles have numerous applications in chemical biology and materials science. Tetrazines most often quench the emission of pendant fluorophores. This effect, however, is diminished upon iedDA, leading to the formation of emissive products with important applications in fluorescence labelling of biomolecules. Herein we investigate the effect of the dienophile on the fluorescence enhancement obtained upon reaction with a tetrazine-quenched fluorophore and study the possible mechanisms of fluorescence quenching by both the tetrazine and its reaction products through a combination of linear and ultrabroadband two-dimensional electronic spectroscopy (2D ES) experiments. The dihydropyridazine product obtained from reaction of the tetrazine with a strained cyclooctene shows a residual fluorescence quenching effect, greater than that exerted by the pyridazine arising from reaction of the tetrazine with the analogous alkyne. Ultrabroadband 2D ES measurements reveal that resonance energy transfer is the mechanism responsible for the fluorescence quenching effect of tetrazines, whereas a mechanism involving more intimate electronic coupling, most likely photoinduced electron transfer, is responsible for the quenching effect of the dihydropyridazine. These studies uncover parameters that can be tuned to maximize fluorogenic efficiency in bioconjugation reactions and they reveal that strained alkenes, though optimal for fast kinetics, are not the best reaction partners for achieving maximum contrast ratio in fluorescence labeling.

Introduction

Inverse electron demand Diels-Alder (iedDA) reactions between s-tetrazines and strained dienophiles[1-3] (Figure 1) have become increasingly widespread, with applications in areas ranging from chemical biology[4-6] to materials science.[7-8] With remarkably fast reaction rates, innocuous byproduct formation, and no catalyst requirement, these transformations offer an excellent alternative to azide-alkyne cycloadditions and other 'click' reactions, especially for bioconjugation reactions performed *in cellulo*.[5] Beyond the remarkable kinetics, an attractive feature of iedDA reactions involving tetrazines is the possibility of obtaining fluorescent products from non-emissive precursors, *i.e.* a fluorogenic reaction, given the right choice of reaction partners.[9-22] This feature can be particularly useful for in situ fluorescence labeling of cellular species to enable their visualization and tracking by various microscopy techniques. The fluorogenic character stems from the strong fluorescence quenching effect that tetrazines can exert on tethered fluorophores, which leads to net fluorescence enhancement once the tetrazine core is broken.

Significant efforts have been devoted to the optimization of reaction partners to increase the rates of iedDA reactions for applications in bioconjugation chemistry.[23] The fluorogenic properties of these transformations, however, have received comparably less attention, despite much room for improvement for applications in which high contrast is important and for techniques like super-resolution imaging. Important work in this area has placed an emphasis on maximizing the fluorescence quenching efficiency of the tetrazine as a means to decrease the brightness of the tetrazine-functionalized reactant, which can result in impressive fluorescence enhancement (turn-on ratio) upon cycloaddition. In this context, recent advances in the design of fluorogenic iedDA substrates based on quenching by through-bond energy transfer (TBET) to tetrazine moieties have resulted in hundred-fold emission enhancements upon

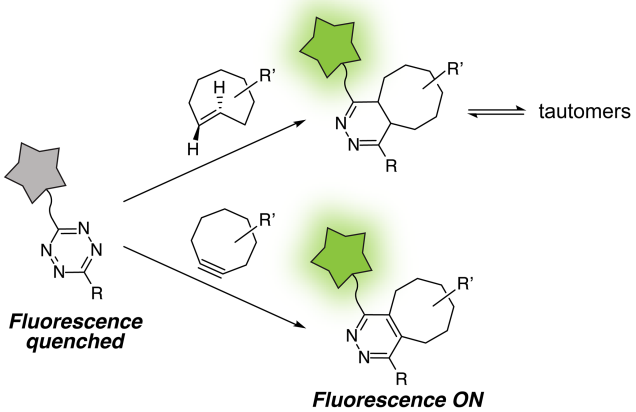

Figure 1. Inverse electron demand Diels-Alder reaction between s-tetrazines and common strained dienophiles. With the right choice of reaction partners, the reaction can be rendered fluorogenic. The mechanism of fluorescence quenching by tetrazines, however, remains speculative.

reaction.[24-31] Yet the mechanism responsible for the general quenching effect of tetrazines on other, commonly used, non-conjugated fluorophores remains speculative, and the influence of the dienophile on the photophysical properties of the iedDA reaction products has been ignored.

In the course of our studies, we have encountered fluorogenic systems in which the fluorescence quantum yield of the iedDA product varies significantly with the choice of dienophile.[32] Furthermore, we and others[25] have found the luminescence quantum yields of the dihydropyridazine-functionalized products to be lower than those of the parent, non-functionalized fluorophores. This difference indicates the presence of non-radiative deactivation pathways that are still in operation in the 'turned-on' products. In this work, we study the fluorescence quenching effect of tetrazines and the products generated in iedDA reactions with various dienophiles, discussing the implications on the design of fluorogenic transformations. We provide evidence for a resonance energy transfer process between a tetrazine and spectrally overlapping fluorophores, and for a more intimate quenching mechanism involving strong electronic coupling between the dihydropyridazine product and the fluorophore, likely electron transfer. These results are significant because they shed light on critical processes that determine the fluorogenic efficiency and the scope of fluorescence labeling reactions based on tetrazine cycloadditions. Furthermore, they offer a unique demonstration of ultrabroadband two-dimensional electronic spectroscopy (2D ES) applied to the study of fluorescence quenching pathways.

Results and Discussion

Intermolecular fluorescence quenching by tetrazines, pyridazines and dihydropyridazines: linear steady state and time-resolved studies

To investigate the effect of the dienophile on the fluorogenic efficiency of iedDA reactions, we began by studying the bimolecular quenching of various fluorophores with increasing concentrations of 3,6-bis(2-hydroxyethyl)-s-tetrazine, **Q1**, or of its reaction products with either a strained alkene or alkyne (**Q2** and **Q3**, respectively, see Figure 2). Although aryl-substituted tetrazines are used in bioconjugation reactions more often than the alkyl-substituted counterparts due to their favorable reaction kinetics and ease of synthesis,[4, 7] we used the alkyl derivatives because they obviate potential influence of the substituents and thereby isolate the quenching effect of the tetrazine moiety. Furthermore, we found **Q1**, and especially its cycloaddition reaction products, to have better solubility than some of the simple aryl tetrazines used in bioconjugation reactions, particularly in aqueous solvent mixtures at the high concentrations required for typical intermolecular quenching experiments (results not shown). Still, because of limitations in solubility at such high concentrations, all quenching studies reported herein were conducted in a 2:1 mixture of acetonitrile/aqueous PBS buffer.

The dialkyl tetrazine used in this study was synthesized from 3-hydroxypropionitrile and hydrazine hydrate with nickel triflate as catalyst (Scheme S1), in a protocol optimized from the method described by Devaraj and coworkes.[25] As dienophiles, we selected *exo*-(*E*)-bicyclo[6.1.0]non-4-en-9-yl-methanol (hereafter trans-cyclooctene, TCO)[33] and the alkyne analogue *exo*-bicyclo[6.1.0]non-4-yn-9-yl-methanol (BCN)[34] to enable direct comparison of the iedDA products.[35] These fused ring systems had been specifically designed to maximize the rate of reaction with tetrazines and are commonly used in ligation applications. Other strained alkenes such as cyclopropenes and their derivatives also have shown favorable kinetics in iedDA reactions with tetrazines, including examples of fluorogenic bioconjugation reactions.[14] As these dienophiles become more broadly used, their effect on the fluorogenic efficiency of the reaction with tetrazines ought to be investigated systematically. The nature of the substituents on the cyclopropene, however, can lead to a wide variety of products[36] that extend beyond the scope of this initial study.

A range of fluorophores covering the visible spectrum (Figure 2) was selected for the quenching studies. The emission profiles of the fluorophores show various degrees of overlap with the absorption profile of the tetrazine **Q1** (Figure 2A and Table 1), enabling the assessment of both Resonance Energy Transfer (RET) and non-RET mechanisms. The cycloaddition products, **Q2** and **Q3**, do not absorb significantly in this region of the spectrum. We sought to work with fluorophores that would have a single species in solution (e.g., a single protonation state) at neutral pH in order to simplify the interpretation of photophysical studies. The coumarin amide derivative, **F2**, was prepared from Coumarin 343 by simple amide coupling procedure with carbonyldiimidazole (CDI) and ethanolamine (Scheme S2). The orange-emitting *p*-methoxystyryl-substituted BODIPY, **F4**, was synthesized from Knoevenagel condensation of 1,3,5,7-tetramethyl BODIPY[37] and *p*-hydroxybenzaldehyde, followed by alkylation of the phenol with dimethylsulfate, as detailed in the Supporting Information (Scheme S3). The product fluorophore shows a main absorption maximum at 568 nm (ε_{568} = 8.5×10^4 M^{-1}cm^{-1}) and emission maximum at 578 nm (Figure S1), with a fluorescence quantum yield Φ = 0.56 in MeCN/PBS. The small Stokes shift is common of BODIPY fluorophores, and the properties of this new derivative are similar to those of related *p*-hydroxystyryl BODIPY dyes, but without the pH dependence of the fluorescence emission that arises from a phenol moiety.[38] Other fluorophores used in this study were obtained from commercial sources (**F1**, **F5**) or synthesized by reported procedures (**F3**[39]).

Results of steady-state quenching experiments of the various fluorophore-quencher combinations are shown in Figure 3, with Stern–Volmer constants summarized in Table 2. Solutions of dihydropyridazine **Q2** and pyridazine **Q3** quenchers were prepared in situ by reaction of the dialkyltetrazine with three equivalents of the corresponding dienophile. Complete conversion to products was confirmed by the disappearance of the characteristic tetrazine absorption band in the visible spectrum (λ_{abs} = 526 nm), as well as by LC-MS analysis. Control quenching experiments without tetrazine were performed to rule out possible quenching effects of the excess dienophile present in the mixtures. No fluorescence quenching was observed with either BCN or TCO alone. The reaction of TCO with tetrazine and all the fluorescence quenching experiments with the product dihydropyridazine **Q2** were performed under anaerobic conditions; nevertheless, we saw no evidence of oxidation to the pyridazine upon exposure to air in the timescale of our experiments.

Concentrations of quenchers ranging from micromolar to low millimolar were employed in order to reach levels of quenching

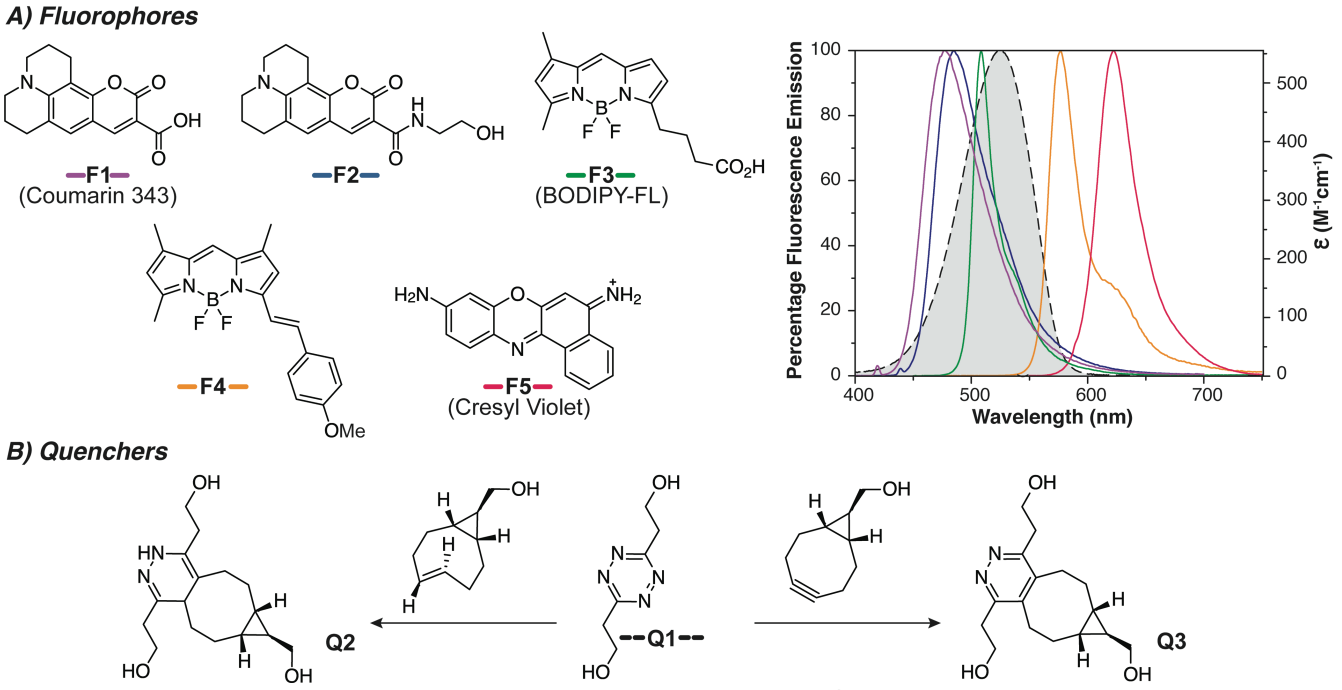

Figure 2. Fluorophores (A) and quenchers (B) selected for this study. Panel in the upper right shows the photoluminescence spectrum of each fluorophore (solid lines, excited at their respective absorption maxima, listed in Table 1) and their overlap with the absorption spectrum of 3,6-bis(2-hydroxyethyl)-s-tetrazine (dashed line, shaded) in a 2:1 MeCN/PBS buffer mixture. The products of iedDA reaction, **Q2** and **Q3**, with alkene and alkyne TCO and BCN, respectively, do not show significant absorption in the same spectral window.

Table 1. Photophysical and electrochemical properties of fluorophores used in this study.[a]

Compound	Absorption maximum λ_{abs} (nm)	Emission maximum λ_{em} (nm)	Φ	J[b] ($\times 10^{13}$ $M^{-1}cm^{-1}nm^4$)	Förster radius[c] (Å)	$E_{(A/A^-)}$ (V vs. SCE)	$E_{(A+/A)}$ (V vs. SCE)	E_{00} (eV)
F1	420	480	0.671(8)	1.271	21.6	-1.381[e]	1.003[f]	2.76
F2	441	487	0.64(2)	1.495	22.0	-1.652[e]	0.890[f]	2.67
F3	504	512	0.98(2)	2.204	25.2	-1.004[e]	1.184[e]	2.45
F4	568d	578	0.560(4)	0.281	16.3	-1.015[e]	0.865[e]	2.17
F5	590	626	0.54(3)	0.011	9.48	-0.18[f,g]	1.280[e,g]	2.03

[a] Optical properties determined in a 2:1 MeCN/PBS buffer mixture at 25 °C. Electrochemical parameters determined in MeCN with 0.1 M Bu_4NPF_6 as supporting electrolyte. Values in parentheses reflect the uncertainty of the last significant figure. Errors correspond to the standard deviation from triplicate measurements. [b] Overlap integral with the fluorophore as donor and **Q1** as energy acceptor. [c] Determined using the dynamic isotropic limit (2/3) for the orientation factor κ^2. [d] Extinction coefficient ε_{568}= 85000 ± 2000 $M^{-1}cm^{-1}$. [e] Either cathodic or anodic peak potential (E_p) for an irreversible peak. [f] Half-wave potential ($E_{1/2}$) for a reversible peak. [g] Values from reference [40].

of the same order of magnitude as those observed for tetrazine-appended fluorophores (intramolecular quenching, *vide infra*), for which the effective molarity of the quencher is much higher. Comparison of steady-state with analogous time-resolved measurements (Figures S2, S3 and Table S1) revealed that, in some cases, the effect of the tetrazine arises from a combination of dynamic (collisional) and static (involving the formation of non-emissive complexes in the ground state) quenching. We did not deconvolute the contributions of the two types of process because most of the available data were collected at relatively low concentrations of quenchers for which static quenching is less prevalent and difficult to quantify accurately. We only report herein the apparent Stern–Volmer constants extracted from steady-state measurements. These values suffice to establish, at least semi-quantitatively, the relative quenching power of the tetrazine and its various reaction products.

As reflected by the Stern–Volmer constants (Table 2), the quenching effect of the tetrazine is much greater than that of its reaction products with various dienophiles, a difference that supports the application of the iedDA reaction for fluorogenic purposes. Intramolecular fluorescence quenching by tetrazines—with a typical absorption band in the 500–550 nm range—has been shown to be highly dependent on the emission wavelength of the linked fluorophores, prompting the proposal of a RET-based quenching mechanism.[9, 41] The lack of solvent dependence on the quenching of geometrically constrained bichromophoric tetrazine-BODIPY systems lent further credence to the proposed RET mechanism over an alternative

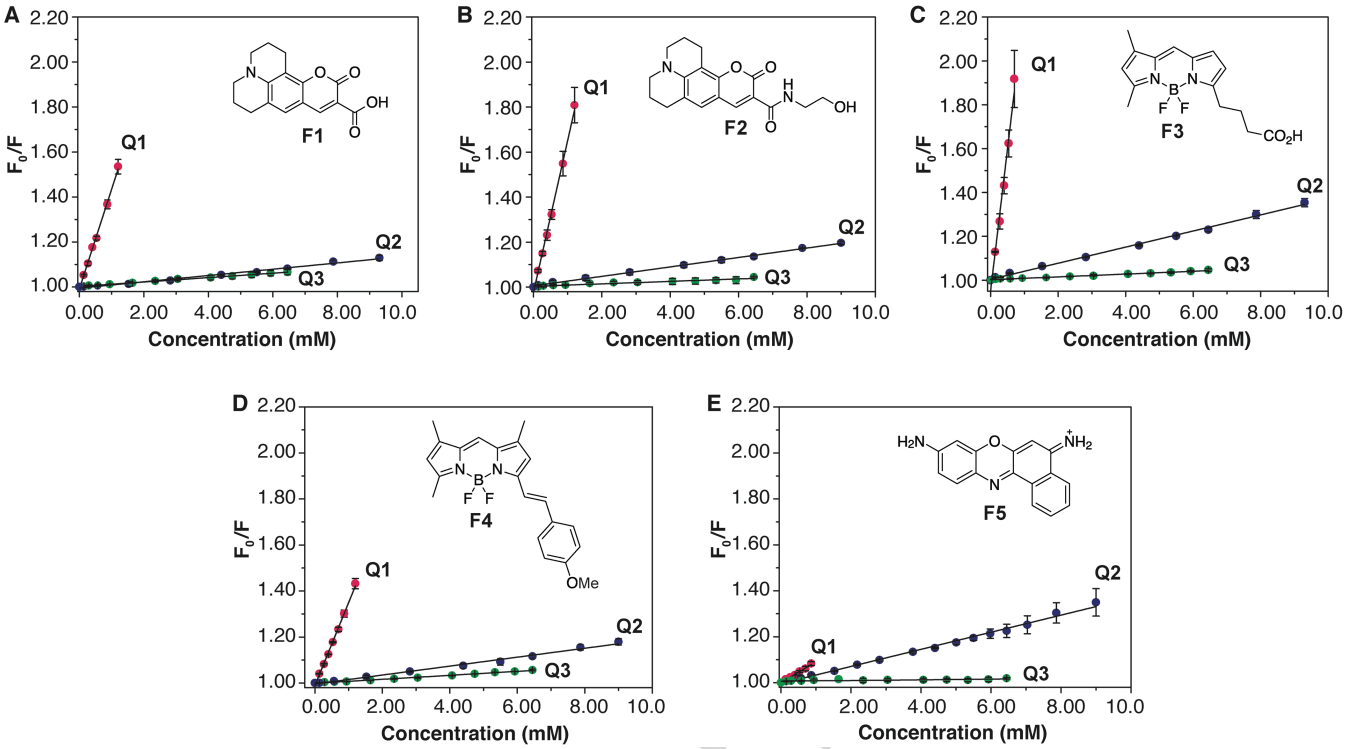

Figure 3. Stern–Volmer plots for fluorophores **F1**-**F5** treated with a dialkyltetrazine (**Q1**), and its reaction products with a strained alkene (**Q2**) or alkyne (**Q3**). Quenching experiments were conducted in a 2:1 MeCN/PBS buffer mixture at 25 °C.

Table 2. Stern–Volmer constants obtained from steady-state fluorescence quenching experiments.

	Q1	Q2	Q3
	K_{SV} (M^{-1})	K_{SV} (M^{-1})	K_{SV} (M^{-1})
F1	440 ± 30	13.9 ± 0.8	10 ± 12
F2	680 ± 70	20.6 ± 0.1	6 ± 2
F3	1200 ± 100	36 ± 2	6 ± 1
F4	360 ± 20	19 ± 1	8.7 ± 0.1
F5	92 ± 9	37 ± 7	1.7 ± 0.9

photoinduced electron transfer (PeT) mechanism.[42] Our results seemed consistent with this notion, with the maximum fluorescence quenching effect observed for the BODIPY FL fluorophore, which exhibits the greatest spectral overlap and longest calculated Förster radius (25.2 Å) with the dialkyltetrazine as energy acceptor (λ_{abs} = 526 nm, ε_{526} = 546 ± 1 $M^{-1}cm^{-1}$). Cresyl Violet—showing almost negligible spectral overlap with the tetrazine—was chosen as a control to support this mechanistic hypothesis. To our surprise, however, this fluorophore was subject to significant quenching by the tetrazine as well. A detailed study of this system, reported elsewhere,[40] ruled out RET and indicated that an excited state proton transfer mechanism operates in this particular case.

For all fluorophores investigated, the extent of fluorescence quenching exerted by the pyridazine **Q3** is almost negligible, whereas that of the dihydropyridazine **Q2** is sizeable. These results indicate that, in the context of fluorogenic labeling, fluorescence emission of tetrazine-functionalized fluorophores will not be fully restored and the maximum possible contrast will not be achieved upon reaction with TCO (*vide infra*). Upon close inspection of the absorption spectrum of the quenchers, a very weak absorption band at 442 nm (ε_{442} = 5.8 $M^{-1}cm^{-1}$) can be observed for **Q2** (Figure S4), thus some contribution from RET to the quenching by this dihydropyridazine cannot be ruled out entirely for the blue-green emitters. The extent of quenching, however, is greater with the orange-red emitting fluorophores, which show very little spectral overlap with this absorption feature. An alternative mechanism is thus most likely involved.

Tetrazines, pyridazines, and dihydropyridazines are electrochemically active and could potentially participate in electron transfer reactions that provide efficient non-radiative pathways for decay of excited fluorophores. In the context of bioorthogonal chemistry, the redox properties of tetrazines—which enable their photocatalytic or electrochemical generation from reversible oxidation of the corresponding dihydrotetrazines—have been exploited to develop methods for controlled activation of bioconjugation reactions at surfaces[43] and in biomaterials.[44] To evaluate the plausibility of fluorescence quenching by a PeT mechanism, we investigated the electrochemical properties of various fluorophores and quenchers used in this study (Figures S5-S11). The main features of the fluorophores are summarized in Table 1. The cyclic voltammogram (CV) of the dialkyltetrazine in acetonitrile with Bu_4NPF_6 as supporting electrolyte displays a reversible reduction peak at $E_{1/2}$ = –0.874 V vs SCE that does not change in shape and intensity after multiple scans. This wave likely corresponds to the reversible formation of a radical anion in the non-aqueous solvent;[42],[45] further reduction to the dianion is not observed in our scan window. A single irreversible oxidation ($E_{p,c}$

= 2.045 V vs SCE) is observed. From these results, photoinduced oxidation of the tetrazine is predicted to be thermodynamically unfavorable for all fluorophores (Table S2),[46] whereas the photoinduced reduction is favorable for all fluorophores except **F5** and thus must be considered still as a feasible quenching mechanism alternative to RET.

The CV of the dihydropyridazine **Q2** in acetonitrile (Figure S11) shows irreversible reduction and oxidation peaks at $E_{p,c}$ = –0.88 V and $E_{p,a}$ = 0.73 V vs. SCE, respectively. Both photoinduced reduction and oxidation of the quencher are thermodynamically favorable with fluorophores **F1** through **F4**, though the photoinduced reduction is more favorable for the coumarins and methoxystyryl BODIPY and the photoinduced oxidation is more favorable for BODIPY FL, **F3**. For cresyl violet, **F5**, only the photoinduced oxidation appears thermodynamically favorable. There is no direct correlation between the redox potentials and the Stern–Volmer constants extracted from bimolecular fluorescence quenching experiments, either from the steady state or time-resolved measurements. Such correlation, however, may be expected in series of structurally related compounds for which the reorganization energy and electronic coupling terms are similar. This is not the case for the compounds studied here, motivating the use of other spectroscopic methods to study the energy transfer mechanisms that apply.

Ultrafast two-dimensional electronic spectroscopy (2D ES) studies

Pump-probe optical spectroscopy techniques yield valuable information about energy transfer mechanisms by selectively exciting an optical transition and probing the time-resolved dynamics of the resultant excited state. The tetrazine and its TCO products, however, are inefficient fluorescence quenchers, and mixtures of fluorophores with tetrazine **Q1** and dihydropyridazine **Q2** returned only transient absorption (TA) spectra that were only subtly different, at best. We therefore utilized an extension of TA spectroscopy, ultrabroadband two-dimensional electronic spectroscopy (2D ES), as a means of resolving weak spectral changes associated with different fluorescence quenching mechanism. The 2D ES technique has a number of advantages over conventional pump-probe spectroscopies. For instance, congested one-dimensional spectra, or samples with multiple chromophores, are readily resolved along the excitation axis in 2D electronic spectra. The technique also avoids an inconvenient trade-off in ultrafast transient absorption, where shorter laser pulses with better time resolution necessitate more excitation bandwidth and decrease excitation specificity. Many of these same advantages informed the development of 2D NMR techniques, and the spectral interpretation of 2D ES proves similar as well.[47-48] Diagonal peaks in 2D ES correspond to individual electronic transitions while off-diagonal cross peaks arise from coupled transitions. The location and evolution of these cross peaks differ based on the underlying energy transfer mechanism.[40, 49] Their examination thus allows one to rule out certain possible fluorescence quenching mechanisms while supporting others.

The 2D ES electronic spectrum of methoxystyryl BODIPY **F4** in 2:1 MeCN:PBS at a waiting time of 100 ps is presented in Figure 4 (expanded and explained in detail in Figure S14). This fluorophore was chosen for further study due to the favorable overlap of the compound's absorption and fluorescence with the excitation bandwidth of the laser (500 – 770 nm). Like in TA spectroscopy, three types of signal contribute to the spectrum. Positive (red) ground state bleach (bleach) and stimulated emission (SE) signals arise from the depletion of the ground state ($S_0 \rightarrow S_1$) by the pump pulse and coherent emission of the first excited state ($S_1 \rightarrow S_0$) to the ground state, respectively. Negative (blue) excited-state absorption (ESA) signal indicates a transition from the first excited state to some higher-lying excited state ($S_1 \rightarrow S_n$), respectively. The bleach and SE signals are comparable to absorption and fluorescence, respectively, while the entire 2D electronic spectrum can be reduced in dimensionality to the equivalent of a TA spectrum by summing along the excitation axis. The inset below the 2D spectrum is the TA spectrum for visual comparison, demonstrating that 2D ES can resolve multiple spectral features that lead to single peaks in TA spectroscopy. Finally, the absorption spectra of methoxystyryl BODIPY **F4** and tetrazine **Q1** are placed on the right inset as additional reference spectra.

Analysis of the 2D electronic spectra after addition of the quenchers enables the evaluation of possible fluorescence quenching mechanisms, including exciton formation, PeT, RET,

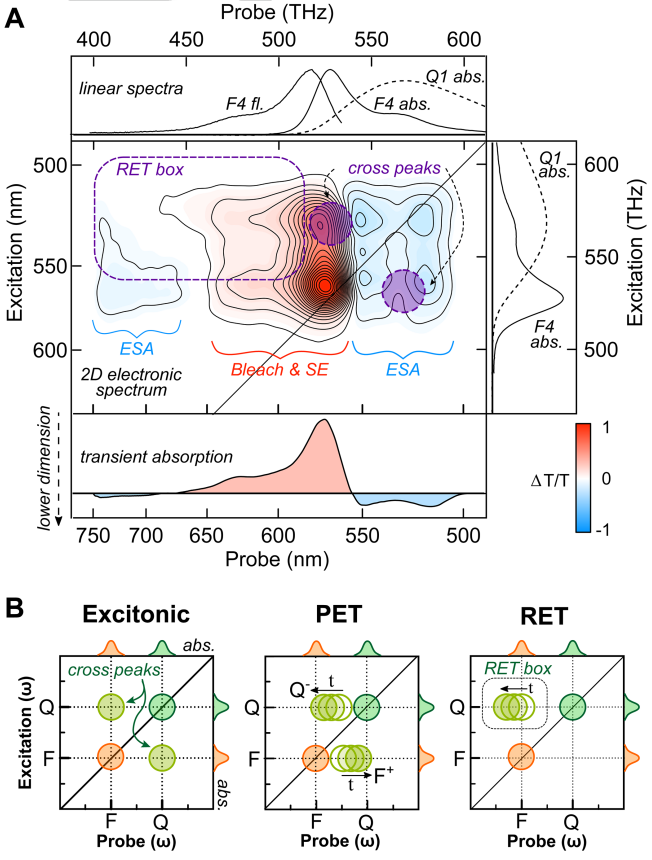

Figure 4. (A) Normalized 2D electronic spectrum of methoxystyryl BODIPY **F4** at a waiting time of 100 ps. Bleach and stimulated emission features appear as red, positive (+) signal, while excited-state absorption features appear as blue, negative (-), signal. Regions marked with dashed violet boxes are areas of mechanistic interest where signatures of RET or excitonic coupling would be expected to appear in the presence of tetrazine **Q1**. Insets to the top, right and bottom include 1D spectra for ease of comparison. (B) Simplified schematic representation of the signature spectral features associated with various possible energy transfer mechanisms between a fluorophore (F, orange) and a quencher (Q, green). The RET box illustrates the region where changes in the spectrum due to RET are likely to occur. In FRET between two fluorophores, the region would likely include the growth of a stimulated emission band. In experiments with a non-emissive acceptor, like those described herein, there would be a loss of stimulated emission from the fluorescent donor and no new peak.

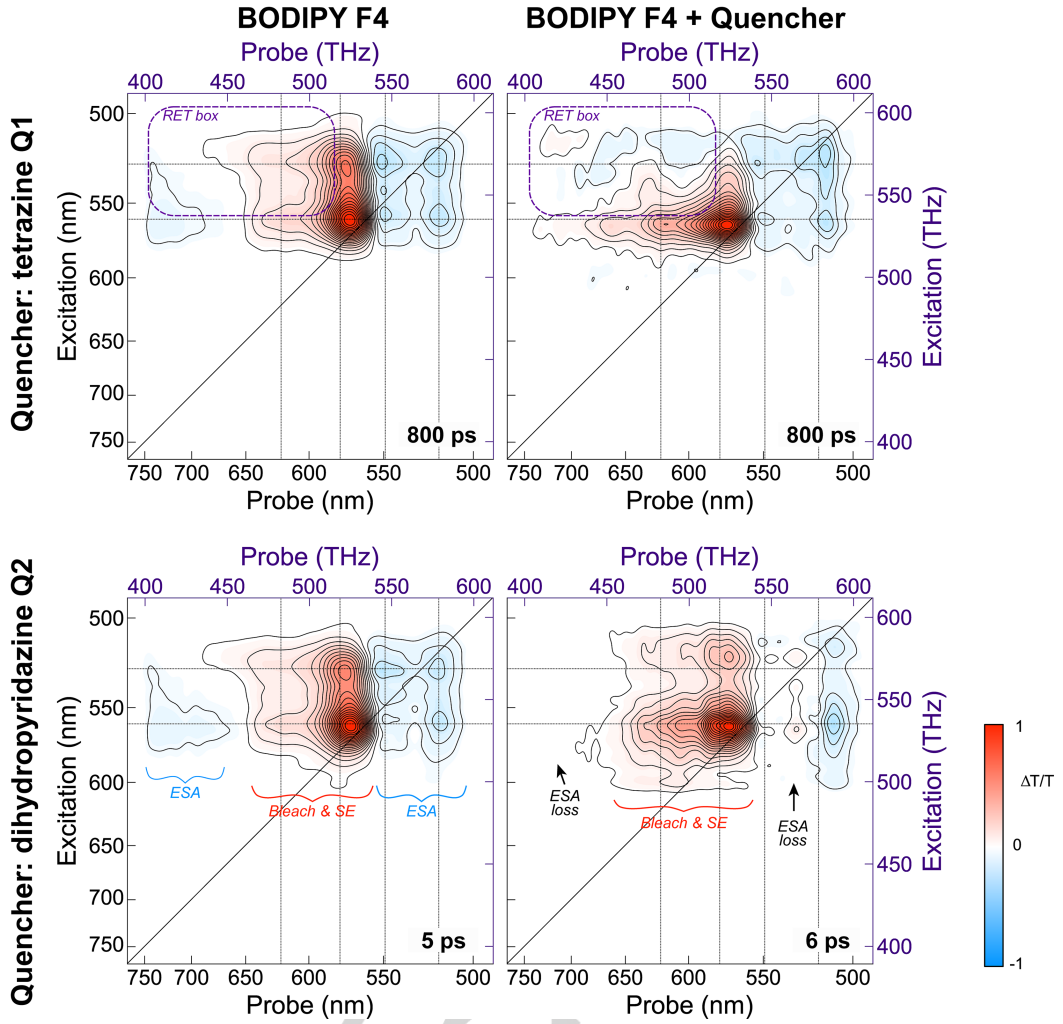

Figure 5. Salient 2D electronic spectra for mechanistic study of methoxystyryl BODIPY, **F4**, treated with tetrazine **Q1** or dihydropyridazine, **Q2**. Horizontal and vertical dashed lines indicate prominent excitation and probe wavelengths in the 2D spectra.

and excited-state proton transfer. Each mechanism has unique 2D ES signatures (Figure 4B), and the latter mechanism was proposed for the fluorescence quenching of cresyl violet by tetrazine **Q1** using a similar analysis.[40] In the case at hand, the BODIPY fluorophore lacks exchangeable protons and therefore only excitonic, PeT, and RET mechanisms need to be considered.

In studies of light-harvesting proteins and nanoparticle assemblies, excitonic coupling leads to cross peaks that appear immediately at common absorption wavelengths, with subsequent energy transfer between chromophores altering the intensity of those cross peaks. Photochemical transformations such as PeT do not lead to the appearance of spectral features with the same immediacy. Nevertheless, new cross peaks at common excitation wavelengths but in a new emission region indicate the alteration of the donor and acceptor electronic states as would be expected for PeT. This new emission feature is associated with the donor–acceptor complex, which can undergo a number of transformations over the course of picoseconds, including back–electron transfer and diffusion.[50-51] The weaker electronic coupling underpinning RET mechanisms yield spectra with a new peak at donor excitation and acceptor emission. This results in a “RET box”, i.e. the area of a 2D electronic spectrum that defines the range of possible excitation energies needed to result in acceptor emissions. In the specific case studied here, the acceptor does not emit appreciable light, thus the energy transfer will likely be indicated by a loss of SE signal of the donor in the RET box.

The 800 ps 2D electronic spectra of methoxystyryl BODIPY **F4** with and without tetrazine **Q1** along with the 5 ps spectra with and without dihydropyridazine **Q2** are presented in Figure 5. Additional 2D spectra at waiting times of 200 fs, 1 ps, 10 ps, and 100 ps are presented in Figures S15 and S16 in the SI. When methoxystyryl BODIPY is exposed to 45 mM (500 equivalents) of tetrazine **Q1**, a comparison of the treated and untreated 2D electronic spectra reveals a reduction in the SE signal in the former for all waiting times. This reduction in SE signal is localized in the high excitation energy region of the 2D spectrum, close to the absorption of tetrazine **Q1** at 525 nm.[52] It should be noted that intermolecular quenching, even at the high concentrations of quencher employed here is not 100% efficient, therefore significant emission signal of the unquenched fluorophore is expected to be present in all of the 2D electronic spectra taken. Furthermore, because neither **Q1** nor **Q2** are emissive, this residual emission from **F4** will be the primary contributor to the 2D spectra.

The absence of cross peaks at the common frequencies of methoxystyryl BODIPY and tetrazine **Q1** eliminates excitonic coupling as a possible mechanism, and the lack of rapidly appearing emission features suggests PeT is a poor fit. In particular, the lack of change in the ESA region of the methoxystyryl BODIPY—where new peaks originating from exciplex or donor-acceptor complex formation would appear—suggests a different mechanism. The area of reduced SE signal in the early time 2D electronic spectra corresponds well to the area indicated by the RET box. Two new ESA features and a third, red-shifted SE peak appear by 800 ps in the area of spectral overlap between **F4** and **Q1**. Both the location and time-scale of the changes[53] suggest that fluorescence quenching by **Q1** proceeds via a RET mechanism. A comparably smaller loss of ESA signal at 525 nm along the excitation line of **F4** may indicate the bleaching of **Q1** due to RET. Under more conventional FRET conditions this bleaching would fall within the RET box; the high energy absorption of **Q1** relative to **F4**, however, results in this alternative placement serving as secondary evidence suggesting a RET mechanism. The long time scale and relatively small quenching efficiency is expected given the relatively small spectral overlap between the two chromophores and their concentrations in solution.

The changes in the 2D spectrum of **F4** in the presence of dihydropyridazine **Q2** proceed much more quickly than in the tetrazine **Q1** case and occur in an entirely different region of the 2D spectrum. Specifically, the ESA features at emission wavelengths between 550 nm and 600 nm disappear by 5 ps but recover partially by 100 ps, with nearly full recovery by 800 ps (Figure S16). The depletion of the ESA features is apparent by 200 fs in the 2D spectra, but close inspection of the transient absorption traces preserved from the phasing process, while noisy, indicate that the treated and untreated methoxystyryl BODIPY are still identical within the noise limit at 100 fs.

As in the case with the tetrazine **Q1**, 2D ES can rule out many of the possible mechanisms of energy transfer in the dihydropyridazine **Q2** system. Fluorescence quenching through RET is unlikely in this case based on the absence of the required spectral overlap between the possible donor and acceptor molecules (**Q2** has an absorption maximum of 341 nm with a shoulder at 430 nm). The rapid disappearance of the BODIPY ESA features by 200 fs suggests a mechanism with stronger electronic coupling than present in a RET mechanism, but the early time transient absorption and the reappearance of ESA signal at 100 ps conflicts with a mechanism based on excitonic coupling. These observations leave PeT as the most likely mechanism for fluorescence quenching by the dihydropyridazine **Q2**. The relatively low efficiency of fluorescence quenching by **Q2** means that the features of the transient species, particularly the BODIPY radical anion, may be covered entirely by the unquenched **F4** signal. Unfortunately, without direct access to the donor-acceptor complex it is impossible to compare the rate of this transient disappearance with the rate of ground state recovery and determine whether the process proceeds through an electron transfer event or through Dexter-type electron exchange. Nevertheless, the time scale of the disappearance and recovery of the ESA features—ultrafast disappearance by 200 fs followed by reappearance over the course of several hundred picoseconds—is consistent with the rates of electron transfer and back electron transfer to the ground state measured by pump-probe spectroscopies in other systems.[54]

Intramolecular fluorescence quenching and fluorogenic iedDA reaction

To assess the impact of the above results on the efficiency of fluorogenic iedDA reactions, we linked covalently the dialkyltetrazine moiety to the BODIPY FL fluorophore **F3** and measured the increase in fluorescence emission upon reaction with either dienophile, TCO or BCN (Figure 6). BODIPY FL was chosen for this experiment because it exhibited the greatest quenching by the tetrazine and potential turn-on upon cycloaddition in our intermolecular studies. As a result, this fluorophore offered a large dynamic range to evaluate the differences in fluorogenic efficiency arising from the two classes of dienophiles studied here. It should be noted, however, that differences in fluorogenic efficiency upon reaction with different dienophiles, leading to pyridazine and dihydropyridazine products, have been observed also with tetrazine-functionalized fluorescein and rhodamine fluorophores widely employed in biolabeling applications.[25]

Treatment of BODIPY FL-Tz with excess alkyne led to a 75-fold fluorescence enhancement, whereas reaction with the alkene only afforded a ~24-fold enhancement. The latter value is comparable to those reported for fluorogenic reactions in similar systems.[9, 14] Oxidation of the dihydropyridazine product to the corresponding pyridazine by treatment with 2,3-dichloro-5,6-dicyanobenzoquinone (DDQ) led to further enhancement of the

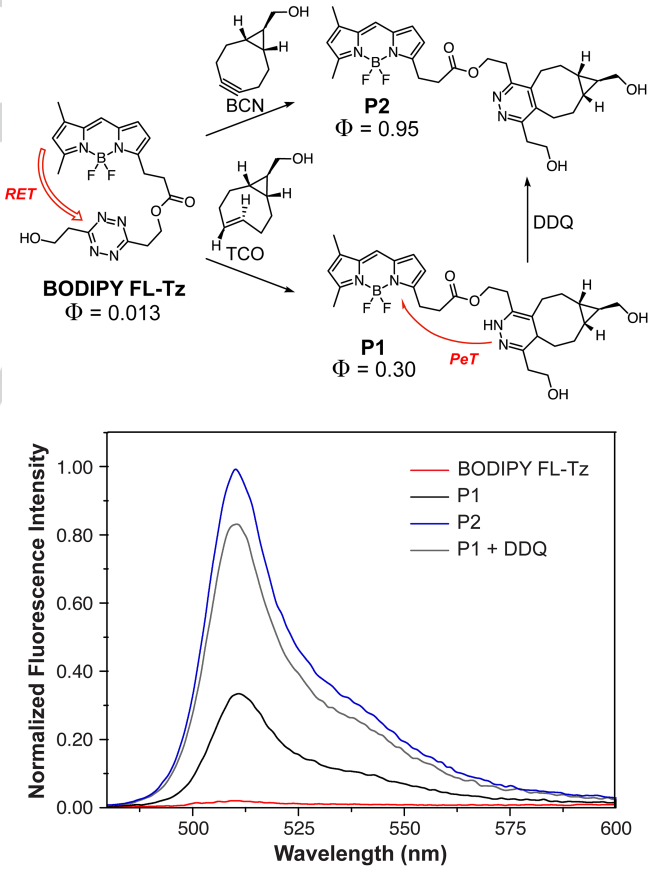

Figure 6. Fluorogenic reaction of tetrazine-functionalized BODIPY with strained dienophiles (only one isomer of the dihydropyridazine product shown). The reaction with the alkyne affords full recovery of the fluorescence whereas that with the alkene does not, due to PeT between the fluorophore and the dihydropyridazine. Fluorescence emission profiles collected after reaction completion, λ_{ex}= 502 nm. Quantum yields determined in 2:1 MeCN/PBS buffer mixture using fluorescein in 0.1 M NaOH as standard (Reference [55]).

fluorescence, but still lower than that observed with the product of the direct reaction with BCN. This small difference in fluorescence emission appears to originate from a quenching effect of the DDQ in the former, as revealed by a control experiment in which an independently prepared sample of the pyridazine product **P2** was treated with excess of the quinone (Figure S17).

Comparison of the quantum yields of the products of the fluorogenic reactions (Figure 6 and Table S3) with that of the parent, non-functionalized BODIPY FL, reveals full restoration of the fluorescence emission of BODIPY FL-Tz upon reaction with BCN. These results are consistent with the trends observed in the bimolecular quenching experiments, in which the quenching effect of dihydropyridazine **Q2** was consistently greater than that of pyridazine **Q3**, and the latter was almost negligible in most cases. They also suggest that bimolecular quenching experiments may be valuable for simple evaluation of reaction partners in the process of optimizing the fluorogenic efficiency of a transformation. Moreover, quantum yields determined in 2:1 MeCN/PBS buffer differ very little from those determined in purely aqueous solvent (Table S3), suggesting that the extent of fluorescence quenching is similar in both and that the conclusions of our studies are relevant to the interpretation of systems operating in typical bioconjugation conditions.

The CV of BODIPY FL-Tz in acetonitrile (Figure S12) shows two reduction waves, one at $E_{1/2}$ = –0.896 V and a second, irreversible one at $E_{p,c}$ = –1.075 V vs SCE. An irreversible oxidation peak was observed at 1.197 V vs. SCE. These features match those of the tetrazine and BODIPY FL measured independently, thus confirming there is no direct electronic communication between the two chromophores. Significantly, the quantum yield of **P1** increases to Φ=0.42 ± 0.02 in 1,2-dichloroethane (ε= 10.36), consistent with a decrease in the rate of photoinduced electron transfer in the solvent of lower dielectric constant.

Conclusion

Inverse electron demand Diels–Alder (iedDA) reactions between tetrazines and strained dienophiles have become increasingly used in bioconjugation chemistry, and their fluorogenic character makes them particularly valuable for labeling and tracking biomolecules in cellulo. Important efforts have been devoted to tailoring reaction partners for improved kinetics, stability, and biocompatibility. In particular, recent design of strained dienophiles—beyond those developed for other click reactions—has led to reaction rates unparalleled by any other bioconjugation reaction to date.

Speed, however, comes at the expense of fluorogenic efficiency. Though strained alkenes offer the fastest kinetics in reactions with tetrazines, our study demonstrates that the product dihydropyridazine can participate in photoinduced electron transfer processes that impact the fluorescence efficiency of pendant fluorophores. The quenching effect of the pyridazine obtained from the strained alkynes, on the other hand, is almost negligible with all the fluorophores included in our study. These observations make strained alkynes a better choice of dienophile for fluorescence labeling applications that demand high contrast and for super-resolution microscopy. Other dienophiles such as norbornene and cyclopropenes must be evaluated further in this context, though the currently available data shows fluorogenic enhancements comparable to those obtained with the strained trans-cyclooctenes.[25] It is important to note that, under oxidizing conditions, the dihydropyridazine can be converted to a pyridazine post ligation, leading to further fluorescence enhancement. Nevertheless, in systems in which the oxidation is not facile or is not easily controlled, the fluorogenic efficiency of reactions with alkenes might be limited or vary over time or sample, thus affecting quantitative analysis.

Two-dimensional electronic spectroscopy reveals the fluorescence quenching mechanism of a dialkyltetrazine to be mainly RET, though PeT is thermodynamically feasible in most cases investigated here.

With new photochemical mechanistic insight, the development of fluorogenic reactions with tetrazines can be approached in a more rational and systematic fashion. One obvious avenue includes the optimization of various parameters affecting RET efficiency in order to decrease the fluorescence emission of the tetrazine-functionalized fluorophore in its 'off' state. Yet consideration of the electrochemical properties of the fluorophores and click reaction products in the design process may enable the tuning of the 'on' state too. Specifically, decreasing the rate of PeT with the dihydropyridazine product can result in greater overall fluorescence enhancement upon bioconjugation. Finally, smart use of the electrochemical properties of the tetrazines themselves may also help in the design of better fluorogenic reactions. For example, careful matching of the fluorophore and tetrazine redox potentials may enable the engineering of fluorogenic transformations based entirely on the modulation of PeT rates rather than RET quenching, thus enabling the use of fluorophores with low energy emission—which lie beyond the range optimal for RET—and expanding the scope of these click reactions in the context of bioimaging applications.

Acknowledgements

This work was supported by the National Science Foundation under grant CHE-1555116 to D.B and CHE-1552235 to D.B.T. D.B.T. also acknowledges support from the Alfred P. Sloan Foundation. W.P.C. acknowledges support from the Margaret Strauss Kramer Fellowship, and B.P.-P. thanks the NSF for a Graduate Research Fellowship under Grant No. DGE1342536. The authors thank Prof. Nicholas Geacintov and Dr. Alexander Durandin for access to equipment and assistance with fluorescence lifetime experiments. They also thank María De Abreu and Dr. Guangqian Zhang for help in the early stages of these studies.

Keywords: Tetrazine • FRET • photoinduced electron transfer • 2D electronic spectroscopy • quenching mechanism

[1] J. Sauer, D. K. Heldmann, J. Hetzenegger, J. Krauthan, H. Sichert, J. Schuster, *Eur. J. Org. Chem.* **1998**, *1998*, 2885-2896.

[2] M. L. Blackman, M. Royzen, J. M. Fox, *J. Am. Chem. Soc.* **2008**, *130*, 13518-13519.

[3] N. K. Devaraj, R. Weissleder, S. A. Hilderbrand, *Bioconj. Chem.* **2008**, *19*, 2297-2299.

[4] J. Šečkutė, N. K. Devaraj, *Curr. Opin. Chem. Biol.* **2013**, *17*, 761-767.

[5] B. L. Oliveira, Z. Guo, G. J. L. Bernardes, *Chem. Soc. Rev.* **2017**, *46*, 4895-4950.

[6] E. Kozma, O. Demeter, P. Kele, *ChemBioChem* **2017**, *18*, 486-501.

[7] A.-C. Knall, C. Slugovc, *Chem. Soc. Rev.* **2013**, *42*, 5131-5142.

[8] J. Escorihuela, A. T. M. Marcelis, H. Zuilhof, *Adv. Mater. Interfaces* **2015**, *2*, 1500135.
[9] N. K. Devaraj, S. Hilderbrand, R. Upadhyay, R. Mazitschek, R. Weissleder, *Angew. Chem.* **2010**, *122*, 2931-2934.
[10] K. Lang, L. Davis, S. Wallace, M. Mahesh, D. J. Cox, M. L. Blackman, J. M. Fox, J. W. Chin, *J. Am. Chem. Soc.* **2012**, *134*, 10317-10320.
[11] K. Lang, L. Davis, J. Torres-Kolbus, C. Chou, A. Deiters, J. W. Chin, *Nat. Chem.* **2012**, *4*, 298-304.
[12] D. S. Liu, A. Tangpeerachaikul, R. Selvaraj, M. T. Taylor, J. M. Fox, A. Y. Ting, *J. Am. Chem. Soc.* **2012**, *134*, 792-795.
[13] T. Plass, S. Milles, C. Koehler, J. Szymański, R. Mueller, M. Wießler, C. Schultz, A. Lemke Edward, *Angew. Chem. Int. Ed.* **2012**, *51*, 4166-4170.
[14] J. Yang, J. Šečkutė, C. M. Cole, N. K. Devaraj, *Angew. Chem.* **2012**, *124*, 7594-7597.
[15] J. Šečkutė, J. Yang, N. K. Devaraj, *Nucleic Acids Res.* **2013**, *41*, e148.
[16] A. Darko, S. Wallace, O. Dmitrenko, M. M. Machovina, R. A. Mehl, J. W. Chin, J. M. Fox, *Chem. Sci.* **2014**, *5*, 3770-3776.
[17] P. N. Asare-Okai, E. Agustin, D. Fabris, M. Royzen, *Chem. Commun.* **2014**, *50*, 7844-7847.
[18] A. M. Pyka, C. Domnick, F. Braun, S. Kath-Schorr, *Bioconj. Chem.* **2014**, *25*, 1438-1443.
[19] P. Agarwal, J. Beahm Brendan, P. Shieh, R. Bertozzi Carolyn, *Angew. Chem.* **2015**, *127*, 11666-11672.
[20] B. L. Oliveira, Z. Guo, O. Boutureira, A. Guerreiro, G. Jiménez-Osés, G. J. L. Bernardes, *Angew. Chem. Int. Ed.* **2016**, *55*, 14683-14687.
[21] E. Németh, G. Knorr, K. Németh, P. Kele, *Biomolecules* **2020**, *10*, 397-.
[22] J. Galeta, R. Dzijak, J. Oborǐl, M. Dračínský, M. Vrabel, *Chem. Eur. J.*, *n/a*.
[23] For selected examples see: (a) Taylor, M. T.; Blackman, M. L.; Dmitrenko, O.; Fox, J. M. *J. Am. Chem. Soc.* **2011**, *133*, 9646-9649. (b) Patterson, D. M.; Nazarova, L. A.; Xie, B.; Kamber, D. N.; Prescher, J. A. *J. Am. Chem. Soc*. **2012**, *134*, 18638-18643. (c) Kamber, D. N.; Nazarova, L. A.; Liang, Y.; Lopez, S. A.; Patterson, D. M.; Shih, H.-W.; Houk, K. N.; Prescher, J. A. *J. Am. Chem. Soc.* **2013**, *135*, 13680-13683. (d) Yang, J.; Liang, Y.; Šečkutė, J.; Houk, K. N.; Devaraj, N. K. *Chem. Eur. J.* **2014**, *20*, 3365-3375. (e) Lambert, W. D.; Scinto, S. L.; Dmitrenko, O.; Boyd, S. J.; Magboo, R.; Mehl, R. A.; Chin, J. W.; Fox, J. M.; Wallace, S. *Org. Biomol. Chem*. **2017**, *15*, 6640-6644.
[24] J. C. T. Carlson, L. G. Meimetis, S. A. Hilderbrand, R. Weissleder, *Angew. Chem.* **2013**, *125*, 7055-7058.
[25] H. Wu, J. Yang, J. Šečkutė, N. K. Devaraj, *Angew. Chem. Int. Ed.* **2014**, *53*, 5805-5809.
[26] L. G. Meimetis, J. C. T. Carlson, R. J. Giedt, R. H. Kohler, R. Weissleder, *Angew. Chem. Int. Ed.* **2014**, *53*, 7531-7534.
[27] G. Knorr, E. Kozma, A. Herner, E. A. Lemke, P. Kele, *Chem. Eur. J.* **2016**, *22*, 8972-8979.
[28] A. Wieczorek, P. Werther, J. Euchner, R. Wombacher, *Chem. Sci.* **2017**, *8*, 1506-1510.
[29] G. Knorr, E. Kozma, J. M. Schaart, K. Németh, G. Török, P. Kele, *Bioconj. Chem.* **2018**, *29*, 1312-1318.
[30] Y. Lee, W. Cho, J. Sung, E. Kim, S. B. Park, *J. Am. Chem. Soc.* **2018**, *140*, 974-983.
[31] A. Kormos, C. Koehler, E. A. Fodor, Z. R. Rutkai, M. E. Martin, G. Mező, E. A. Lemke, P. Kele, *Chem. Eur. J.* **2018**, *24*, 8841-8847.
[32] J. J. Gruskos, G. Zhang, D. Buccella, *J. Am. Chem. Soc.* **2016**, *138*, 14639-14649.
[33] M. T. Taylor, M. L. Blackman, O. Dmitrenko, J. M. Fox, *J. Am. Chem. Soc.* **2011**, *133*, 9646-9649.
[34] J. Dommerholt, S. Schmidt, R. Temming, L. J. A. Hendriks, F. P. J. T. Rutjes, J. C. M. van Hest, D. J. Lefeber, P. Friedl, F. L. van Delft, *Angew. Chem. Int. Ed.* **2010**, *49*, 9422-9425.
[35] It should be noted that strain promoted Diels-Alder reactions between tetrazines and 3-substituted cyclooctynes, also used often in chemical biology, were reported to be normal and not inverse electron demand. See J. A. Wagner, D. Mercadante, I. Nikić, E. A. Lemke, F. Gräter, *Chem. Eur. J*. **2015**, *21*, 12431-12435
[36] D. M. Patterson, L. A. Nazarova, B. Xie, D. N. Kamber, J. A. Prescher, *J. Am. Chem. Soc.* **2012**, *134*, 18638-18643.
[37] L. Wu, K. Burgess, *Chem. Commun.* **2008**, 4933-4935.
[38] T. Bura, P. Retailleau, G. Ulrich, R. Ziessel, *J. Org. Chem.* **2011**, *76*, 1109-1117.
[39] K. Gießler, H. Griesser, D. Göhringer, T. Sabirov, C. Richert, *Eur. J. Org. Chem.* **2010**, *2010*, 3611-3620.
[40] W. P. Carbery, B. Pinto-Pacheco, D. Buccella, D. B. Turner, *J. Phys. Chem. A* **2019**, *123*, 5072-5080.
[41] D. Kim, J.-H. Lee, J. Y. Koo, H. M. Kim, S. B. Park, *Bioconj. Chem.* **2020**, *31*, 1545-1550.
[42] C. Dumas‐Verdes, F. Miomandre, E. Lépicier, O. Galangau, T. Vu Thanh, G. Clavier, R. Méallet‐Renault, P. Audebert, *Eur. J. Org. Chem.* **2010**, *2010*, 2525-2535.
[43] F. Ehret, H. Wu, S. C. Alexander, N. K. Devaraj, *J. Am. Chem. Soc.* **2015**, *137*, 8876-8879.
[44] H. Zhang, W. S. Trout, S. Liu, G. A. Andrade, D. A. Hudson, S. L. Scinto, K. T. Dicker, Y. Li, N. Lazouski, J. Rosenthal, C. Thorpe, X. Jia, J. M. Fox, *J. Am. Chem. Soc.* **2016**, *138*, 5978-5983.
[45] The reduction peak in the CV of other disubstituted tetrazines has been described as an electrochemically irreversible but chemically reversible two-electron process leading to the protonated dianion, by analogy to the electrochemical behavior of quinone systems. This description is more appropriate for electrochemical data acquired in protic solvents. See Ref. 43 and Qing, Z.; Audebert, P.; Clavier, G.; Miomandre, F.; Tang, J.; Vu, T. T.; Méallet-Renault, R. *J. Electroanal. Chem*. **2009**, *632*, 39-44.
[46] Standard free energies for the photoinduced electron transfer step were estimated using the Rehm-Weller equation. The work term is negligible in solvents of high dielectric constant such as those used in this study. See: Kavarnos, G. J.; Turro, N. *J. Chem. Rev*. **1986**, *86*, 401-449
[47] J. D. Hybl, A. W. Albrecht, S. M. Gallagher Faeder, D. M. Jonas, *Chem. Phys. Lett.* **1998**, *297*, 307-313.
[48] D. M. Jonas, *Science* **2003**, *300*, 1515-1517.
[49] G. D. Scholes, T. Mirkovic, D. B. Turner, F. Fassioli, A. Buchleitner, *Energy Environ. Sci.* **2012**, *5*, 9374-9393.
[50] A. H. Zewail, in *Femtochemistry: Ultrafast Dynamics of the Chemical Bond*, World Scientific Publishing Company, **1994**, pp. 3-22.
[51] C. Consani, G. Auböck, F. van Mourik, M. Chergui, *Science* **2013**, *339*, 1586.
[52] The observed reduction in SE signal is not the result of simple overlap with opposite sign ESA signal from the tetrazine **Q1**, because the molar absorptivity of the latter is very low. At pump powers five times greater than that used in this experiment the measured 2D signal for the tetrazine was still barely distinguishable from noise, thus the 2D spectrum is not included here. Yet at high concentrations, the tetrazine **Q1** absorbs significant laser light and could cause an inner-filter effect in the 2D spectra. To rule out this effect, we inspected the ratio between the high and low excitation peaks in the ESA region and observed no change with and without tetrazine **Q1**.
[53] B. K. Petkov, T. A. Gellen, C. A. Farfan, W. P. Carbery, B. E. Hetzler, D. Trauner, X. Li, W. J. Glover, D. J. Ulness, D. B. Turner, *Chem* **2019**, *5*, 2111-2125.
[54] P. A. van Hal, R. A. J. Janssen, G. Lanzani, G. Cerullo, M. Zavelani-Rossi, S. De Silvestri, *Chem. Phys. Lett.* **2001**, *345*, 33-38.
[55] A. M. Brouwer, *Pure Appl. Chem.* **2011**, *83*, 2213-2228.

10.1002/ange.202008757

Entry for the Table of Contents

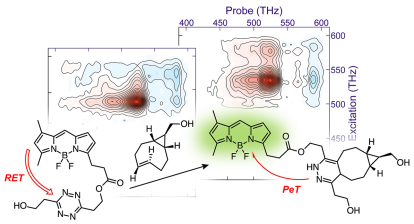

An ultrafast look at fluorogenic tetrazines. Two-dimensional electronic spectroscopy and electrochemical studies provide mechanistic insight on the fluorescence quenching effects of tetrazines and their Diels-Alder cycloaddition products. The studies uncover the influence of the dienophile on the fluorogenic efficiency of reactions with tetrazine-decorated fluorophores and reveal options for maximizing contrast in biolabeling applications.